



Article ID 1007-1202(2025)03-0213-09 DOI <https://doi.org/10.1051/wujns/2025303213>

Cite this article: WANG Zechuan, ZHANG Zhenhua, CHENG Shaowei, *et al.* Study on the Effect of Spot Size and Non-Linearity on PSD Positioning Accuracy[J]. *Wuhan Univ J of Nat Sci*, 2025, 30(3): 213-221.

Study on the Effect of Spot Size and Non-Linearity on PSD Positioning Accuracy

□ WANG Zechuan¹, ZHANG Zhenhua^{1†}, CHENG Shaowei¹, YANG Haima², HUANG Bo¹, LIU Jin¹

1. School of Electronic and Electrical Engineering, Shanghai University of Engineering Science, Shanghai 201620, China;

2. School of Optical-Electrical and Computer Engineering, University of Shanghai for Science and Technology, Shanghai 200093, China

Abstract: Position-sensitive detector (PSD) is widely used in precision measurement fields such as flatness detection, auto-collimator systems, and degrees of freedom testing. However, due to factors such as uneven surface resistance and differences in electrode structures, the nonlinearity of PSD becomes increasingly severe as the photosensitive surface moves from the center toward the edges of the four electrodes. To address this issue, a PSD nonlinearity correction algorithm is proposed. The algorithm utilizes the particle swarm optimization (PSO) algorithm to determine the optimal weights and thresholds, providing better initial parameters for the back propagation (BP) neural network. The BP neural network then iterates continuously until the error conditions are met, completing the correction process. Furthermore, a PSD nonlinearity correction system was developed, and the influence of different spot sizes on PSD positioning accuracy was simulated based on the current equation under the Gaussian spot model. This validated the robustness of the correction algorithm under varying spot sizes. The results demonstrate that the overall optimized error is reduced by 84.51%, and for spot sizes smaller than 1 mm, the error reduction exceeds 93.89%. This method not only meets the measurement accuracy requirements but also extends the measurement range of PSD.

Key words: position-sensitive detector; particle swarm algorithm; nonlinear optimization; spot characteristics; positioning accuracy

CLC number: TP399

0 Introduction

Position-sensitive detectors (PSDs) are current-distributing photoelectric devices with a continuous photosensitive surface, capable of rapidly responding to the centroid position of a light spot irradiated on their surface. Due to their high positional resolution, simple signal processing, and excellent measurement continuity, PSDs are widely applied in scenarios with stringent real-

time requirements, such as flatness detection^[1], real-time coaxiality measurement^[2], and robotic arm trajectory monitoring^[3].

In 1960, Lucovsky *et al*^[4] derived a differential equation describing the photoelectric potential distribution of a two-dimensional planar P-N junction based on the continuity equation of carriers, thereby establishing the theoretical foundation for PSD modeling. Despite their advantages of fast response speed and high resolu-

Received date: 2024-12-02 © Wuhan University 2025

Foundation item: Supported by the National Natural Science Foundation of China (U1831133); Open Fund of Key Laboratory of Space Active Optoelectronics Technology, Chinese Academy of Sciences (2021ZDKF4)

Biography: WANG Zechuan, male, Master candidate, research direction: 3D measurement. E-mail: zechuan17@163.com

† Corresponding author. E-mail: zhenhuazhang1985@163.com

This is an Open Access article distributed under the terms of the Creative Commons Attribution License (<https://creativecommons.org/licenses/by/4.0>), which permits unrestricted use, distribution, and reproduction in any medium, provided the original work is properly cited.

tion, PSDs are significantly affected by the non-uniformity of surface resistance and substantial interference between electrodes, which severely degrade the detector's linearity. Since PSDs measure the intensity of incident light spots, the size of the laser spot and the effectiveness of subsequent nonlinear optimization directly determine measurement accuracy. Wang *et al*^[5] proposed a neural network-based correction approach for PSD, establishing a mapping between actual output and spot position with a limited dataset, which resulted in highly linear signals over a wide range. Shang *et al*^[6] investigated various light source scanning methods and concluded that the scanning method under steady-state illumination more accurately reflects the position information of the incident light. Li *et al*^[7] analyzed the impact of light source modes on PSD positioning accuracy, identifying spot radius and position as the primary influencing factors. Huang *et al*^[8] demonstrated that processing PSD output signals under strong background light interference can effectively improve the spatial accuracy of flashpoint position measurements. Zhang *et al*^[9] developed a PSD nonlinear correction method based on the BP optimization algorithm, demonstrating strong generalization ability and feasibility in resolving PSD nonlinearity by fitting actual and ideal position data using a BP neural network. Wang *et al*^[10] corrected the nonlinear distortion of PSD using an improved bicubic interpolation method, achieving favorable results even under dynamic spot conditions.

Building upon this prior research, this paper derives a two-dimensional PSD positioning model under varying spot sizes within a Gaussian spot framework, based on the mathematical model of the Lucovsky differential equation. A nonlinear optimization method combining the Particle Swarm Optimization (PSO) algorithm and the BP neural network is proposed. By correcting measurement errors based on the relationship between input and output values, the proposed method yields predicted values that approximate the true coordinates. Additionally, the effects of different spot sizes on positioning accuracy are analyzed, providing practical insights for improving PSD measurement accuracy.

1 Principle of PSD

A position-sensitive detector (PSD) is a spot position detector based on the semiconductor lateral photoelectric effect. Its structure consists of a P-I-N junction

formed by P-type, N-type semiconductors, along with a high-resistance I layer^[11]. Figure 1 shows the basic structure of a pillow-shaped two-dimensional PSD, which is an improved version of a quadrilateral PSD. The top surface of the pillow-shaped PSD is a photosensitive surface with arc-shaped electrodes, while the four sides are connected to four current output terminals symmetrically drawn from the arc-shaped edges. The bottom surface has a common cathode. The four current output terminals, X_1 , X_2 , Y_1 , and Y_2 , collect different currents generated by the distances between the spot centroid incident on the photosensitive surface and the respective electrodes. By calculating these currents, the position coordinates of the spot can be determined. The common cathode is used to apply a reverse bias voltage during operation to achieve ideal linearity.

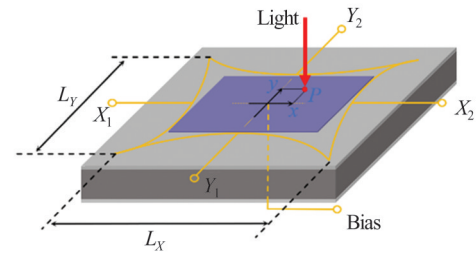


Fig. 1 Pillow-type PSD structure model

When incident light projects onto the photosensitive surface of the PSD, forming a light spot, the lateral photoelectric effect converts the incident light into photocurrent. The output current intensities at the four electrode terminals correspond to the x and y coordinates of the spot centroid. Using the following equations, the coordinate equations with the photosensitive surface center as the origin^[12] can be calculated:

$$\begin{cases} x = \frac{(U_{X_2} + U_{Y_1}) - (U_{X_1} + U_{Y_2})}{U_{X_1} + U_{Y_1} + U_{X_2} + U_{Y_2}} \times \frac{L_X}{2} \\ y = \frac{(U_{X_2} + U_{Y_2}) - (U_{X_1} + U_{Y_1})}{U_{X_1} + U_{Y_1} + U_{X_2} + U_{Y_2}} \times \frac{L_Y}{2} \end{cases} \quad (1)$$

where U_{X_1} , U_{X_2} , U_{Y_1} , U_{Y_2} are the voltage values obtained by the four current output electrodes after converting the voltage signals by photocurrent and amplifying them, L_X and L_Y are the two side lengths of the 2D PSD photosensitive surface, respectively, and $L_X = L_Y$ is usually used.

2 Nonlinear Optimization of PSD

2.1 Causes of Nonlinearity

The structure of the pillow-shaped two-dimensional

PSD consists of a single-sided resistive layer for current distribution. In equation (1), the electrode junctions of the pillow-shaped two-dimensional PSD are considered idealized in terms of shape and size. However, due to manufacturing process limitations, the PN junction material of the PSD cannot ensure a uniform distribution of the resistive layer. As a result, the output electrodes often exhibit variations in size and shape, leading to a non-linear relationship between the detected light spot position coordinates and the actual PSD output during measurement. This nonlinearity increases with the distance from the center of the photosensitive surface. Consequently, the photosensitive surface of the PSD is typically divided into two regions: Zone A and Zone B. Zone A is defined as the area within a diameter that is 40% of the boundary length of the photosensitive surface centered on its center, while Zone B covers the region between 40% and 80% of the boundary length. The positional accuracy in Zone A is superior to that in Zone B. Therefore, when it is necessary to use the entire photosensitive surface to expand the measurement range without compromising accuracy, it is essential to correct for the nonlinearity of the PSD.

2.2 PSO-BP Neural Network

A BP (back propagation) neural network is a multi-layer feedforward neural network that uses error back-propagation. The structure of the neural network includes an input layer, hidden layers, and an output layer. The relationship between the output and input can be seen as a mapping. This mapping is obtained through the transfer functions between the input layer and the hidden layer, the hidden layers and the hidden layers, and the hidden layer and the output layer^[13]. The BP neural network, with its robust nonlinear modeling capability, self-learning and adaptive characteristics, strong generalization ability, and proficiency in handling multivariable inputs, serves as an optimal choice for addressing the nonlinear challenges in PSD analysis.

Due to the BP neural network's excessive reliance on the initial weights and thresholds, it often suffers from poor generalization ability and is prone to getting stuck in local optima. To enhance the effectiveness of the algorithm, a particle swarm optimization (PSO) algorithm is introduced. The PSO algorithm, proposed by Kennedy and Eberhart, is a parallel optimization algorithm inspired by the collective behavior of bird flocks

The specific steps are as follows:

and fish schools in nature^[14]. It is a powerful global optimization algorithm with advantages such as strong global search capability, no need for gradient information, the ability to perform multi-objective optimization, and the ability to balance global and local optima. Similar to the genetic algorithm (GA), PSO incorporates the concept of interacting populations. In many applications, PSO has been demonstrated to converge more rapidly to the optimal solution compared with GA^[15]. The PSO has N individual particles combining self-experience and social experience, and the corresponding position of each particle is a solution. The first i particle ($i=1, 2, \dots, N$) starts "flying" in the M -dimensional search space at a random position with a certain speed, and its position and speed are expressed as $X_i=(x_i^1, x_i^2, \dots, x_i^M)$ and $V_i=(v_i^1, v_i^2, \dots, v_i^M)$, which moves towards the optimal solution in the search space, and finally reaches the global optimum. The positions and velocities are updated from generation j to generation $j+1$ as follows:

$$\begin{aligned} V_i(j+1) &= wV_i + c_1r_1(j)[P_p(j) - X_i(j)] \\ &+ c_2r_2(j)[P_g(j) - X_i(j)], \\ X_i(j+1) &= X_i(j) + V_i(j+1), \end{aligned} \quad (2)$$

where w is the inertia weights to regulate the global search, c_1 and c_2 are the individual learning coefficients and the sociological coefficients respectively, r_1 and r_2 are the random numbers within the range of $[0, 1]$ in the iterative process, and P_p and P_g generate the individual optimal solution and the global optimal solution through each update.

However, the standard PSO algorithm tends to exhibit rapid population convergence due to large inertia in the early stages, making it prone to getting trapped in local optima. To balance global and local search capabilities, dynamically adjusted inertia weights w are used during the search process. Shi *et al.*^[16] proposed a linearly decreasing inertia factor:

$$w = w_{\max} - \frac{w_{\max} - w_{\min}}{j_{\max}} \times j, \quad (3)$$

where w_{\max} and w_{\min} are the initial and final values of the inertia factor, j is the current number of iterations, and j_{\max} is the final number of iterations.

Compared with the BP neural network, the PSO algorithm exhibits superior global search capabilities. The process of using PSO to optimize the BP neural network is shown in Fig. 2.

1) Initialize the parameters of the BP neural net-

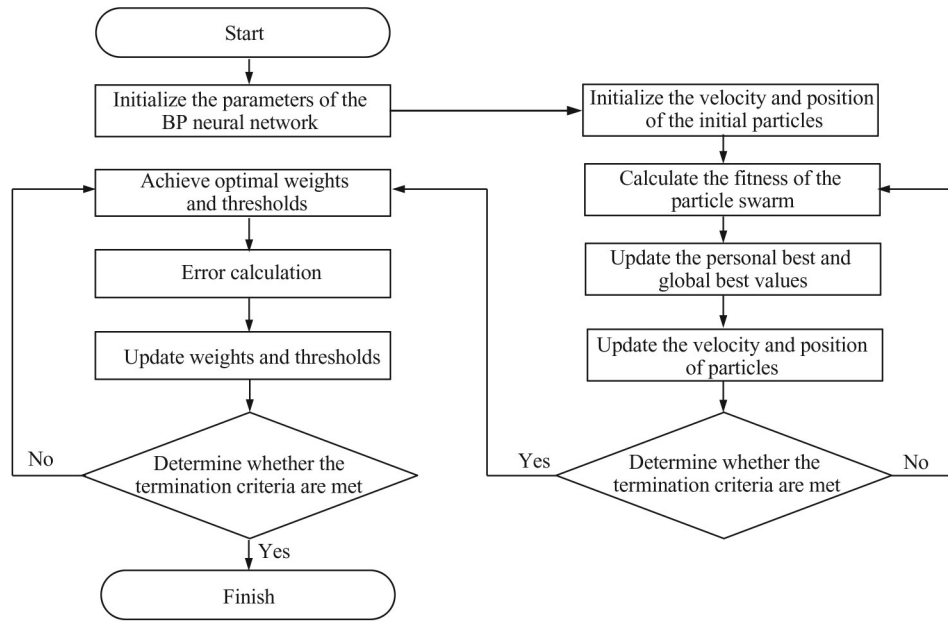


Fig. 2 Flow chart of PSO-BP model

work, including setting the weights and thresholds.

2) Initialize the parameters of the PSO, including setting the population size, initial velocity, and position of the particles.

3) Calculate the fitness of the particles, generating individual best and global best values.

4) Update the velocity and position of the particles based on the individual best and global best values. If the stopping criterion is met, proceed to step 5); otherwise, return to step 3) and repeat.

5) Use the optimized weights and thresholds obtained from the PSO to initialize the BP neural network.

6) Compute the error through the neural network and continuously update the weights and thresholds.

7) Check if the error meets the specified requirements. If not, return to step 6) and continue until the stopping criterion is met, then terminate the training.

3 The Effect of Spot Size on PSD Accuracy

Since the PSD photosensitive surface receives the coordinates of the incident light spot's center of gravity, and the size of the photosensitive surface is limited, the nonlinearity increases as it approaches the edges of the photosensitive surface^[17]. Therefore, it is essential to study the impact of different sizes of incident light spots

on positioning accuracy. According to the Lucovsky differential equation, under the ideal condition where the spot energy is converted to photocurrent without loss, the potential at the point (x, y) on the photosensitive surface can be expressed as:

$$\nabla^2 U(x, y) = -\frac{\rho_d}{\omega_d} I_s(x, y), \quad (4)$$

where $U(x, y)$ represents the potential at the light spot detected on the photosensitive surface, ∇^2 denotes the Laplace operator, ρ_d is the resistivity of the P layer, ω_d is the thickness of the P layer, $I_s(x, y)$ is the total photocurrent at the light spot (x, y) , and the currents at the four electrodes of the PSD can be calculated by the following equations:

$$\begin{cases} I_{x_i}(x, y) = (-1)^{i+1} \frac{\omega_d}{\rho_d} \int_0^L \frac{\partial U(x, y)}{\partial x_i} dy_j, i = 1, 2 \\ I_{y_j}(x, y) = (-1)^{j+1} \frac{\omega_d}{\rho_d} \int_0^L \frac{\partial U(x, y)}{\partial y_j} dx_i, j = 1, 2 \end{cases} \quad (5)$$

where x_i and y_j are the electrode currents, L is the length of the edge electrodes on the PSD's photosensitive surface. Assuming the boundary length of the PSD is one standard unit and taking the center of the PSD's photosensitive surface as the coordinate origin, the junction potential equation can be derived from partial differential equation (4) under the condition of zero electrode potential:

$$U(x, y) = \frac{\rho_d}{\omega_d} \sum_{m=-\infty}^{+\infty} \sum_{n=-\infty}^{+\infty} \times \left[\iint_D \left(I_s(x_1, y_1) \times \frac{\sin(m\pi x) \sin(n\pi y) \sin(m\pi x_1) \sin(n\pi y_1)}{(m^2 + n^2)\pi^2} \right) dx_1 dy_1 \right], \quad (6)$$

where D is the effective area of the 2D PSD photosensitive surface, and the polar coordinate transformation of (6) is performed:

$$U(x, y) = \frac{I_0 \rho_d}{\omega_d} \sum_{m=-\infty}^{+\infty} \sum_{n=-\infty}^{+\infty} \left[\int_{r=0}^{+\infty} \int_{\theta=0}^{2\pi} \left(\frac{\sin(m\pi x) \sin(n\pi y)}{(m^2 + n^2)\pi^2} \times \sin(m\pi(x_0 + r \cos \theta)) \right. \right. \\ \left. \left. \times \sin(n\pi(y_0 + r \cos \theta)) r \exp\left(-\frac{r^2}{w^2}\right) d\theta dr \right) \right]. \quad (7)$$

Available after integrating θ :

$$U(x, y) = \frac{2\pi I_0 \rho_d}{\omega_d} \sum_{m=-\infty}^{+\infty} \sum_{n=-\infty}^{+\infty} \left[\int_{r=0}^{+\infty} \frac{\sin(m\pi x) \sin(n\pi y) \sin(m\pi x_0) \sin(n\pi y_0)}{(m^2 + n^2)\pi^2} \right. \\ \left. \times r \exp\left(-\frac{r^2}{w^2}\right) J_0(m\pi r) J_0(n\pi r) + 2 \sum_{t=1}^{+\infty} (-1)^t (J_{2t}(m\pi r) J_{2t}(n\pi r)) dr \right], \quad (8)$$

where J_{2t} denotes the Bessel function and the Bessel function formula is as follows:

$$r \exp\left(-\frac{r^2}{w^2}\right) J_{2t}(m\pi r) J_{2t}(n\pi r) = \frac{1}{2} w^2 \exp\left(-\frac{(m^2 + n^2)\pi^2 w^2}{4}\right) I_{2t}\left(\frac{mn\pi^2 w^2}{2}\right), \quad (9)$$

$$I_0\left(\frac{mn\pi^2 w^2}{2}\right) + 2 \sum_{t=1}^{+\infty} (-1)^t I_{2t}\left(\frac{mn\pi^2 w^2}{2}\right) = 1, \quad (10)$$

where I_{2t} denotes the modified Type I Bessel function, and the potential is calculated by solving the integral over r :

$$U(x, y) = \frac{2\pi I_0 \rho_d}{\omega_d} \sum_{m=-\infty}^{+\infty} \sum_{n=-\infty}^{+\infty} \left[\int_{r=0}^{+\infty} \frac{\sin(m\pi x) \sin(n\pi y) \sin(m\pi x_0) \sin(n\pi y_0)}{(m^2 + n^2)\pi^2} \times \frac{w^2}{2} \exp\left(-\frac{(m^2 + n^2)\pi^2 w^2}{4}\right) \right]. \quad (11)$$

From this, the current equations for the four electrodes can be calculated:

$$\left\{ \begin{array}{l} I_{x1} = I_0 \sum_{m=-\infty}^{+\infty} \sum_{n=-\infty}^{+\infty} \frac{n \sin(m\pi x_0) \sin(n\pi y_0) [1 - \cos(n\pi)]}{m(m^2 + n^2)\pi^2 b_{m,n}}, \\ I_{x2} = I_0 \sum_{m=-\infty}^{+\infty} \sum_{n=-\infty}^{+\infty} \frac{n \sin(m\pi x_0) \sin(n\pi y_0) [1 - \cos(n\pi)]}{(-1)^{n+1} m(m^2 + n^2)\pi^2 b_{m,n}}, \\ I_{y1} = I_0 \sum_{m=-\infty}^{+\infty} \sum_{n=-\infty}^{+\infty} \frac{m \sin(m\pi x_0) \sin(n\pi y_0) [1 - \cos(m\pi)]}{n(m^2 + n^2)\pi^2 b_{m,n}}, \\ I_{y2} = I_0 \sum_{m=-\infty}^{+\infty} \sum_{n=-\infty}^{+\infty} \frac{m \sin(m\pi x_0) \sin(n\pi y_0) [1 - \cos(m\pi)]}{(-1)^{m+1} n(m^2 + n^2)\pi^2 b_{m,n}}, \end{array} \right. \quad (12)$$

$$\text{where } b_{m,n} = \frac{2}{w^2} \exp\left[\frac{(m^2 + n^2)\pi^2 w^2}{4}\right].$$

To analyze the impact of different spot sizes on the photosensitive surface on the positioning accuracy, a simulation experiment was designed to simulate the calculation of position coordinates under varying spot sizes. The photocurrent I_0 was set to one unit, and the length of the photosensitive surface L was assumed to be nine units. The spot moved across the PSD photosensitive surface with a step size of 0.5 units, simulating four different spot sizes: $w=0.05$, $w=0.10$, $w=0.15$, and $w=0.20$, generating a 17×17 grid of discretized data points, totaling 289 position coordinates. The distribution of the simulated position coordinates for the different spot sizes is shown in Fig. 3.

As shown in the figure, within the Zone A of the photosensitive surface, different spot sizes exhibit good linearity. However, in the Zone B, significant non-linear phenomena are observed due to edge current effects. Additionally, as the spot size increases, the positioning accuracy of the PSD photosensitive surface significantly decreases.

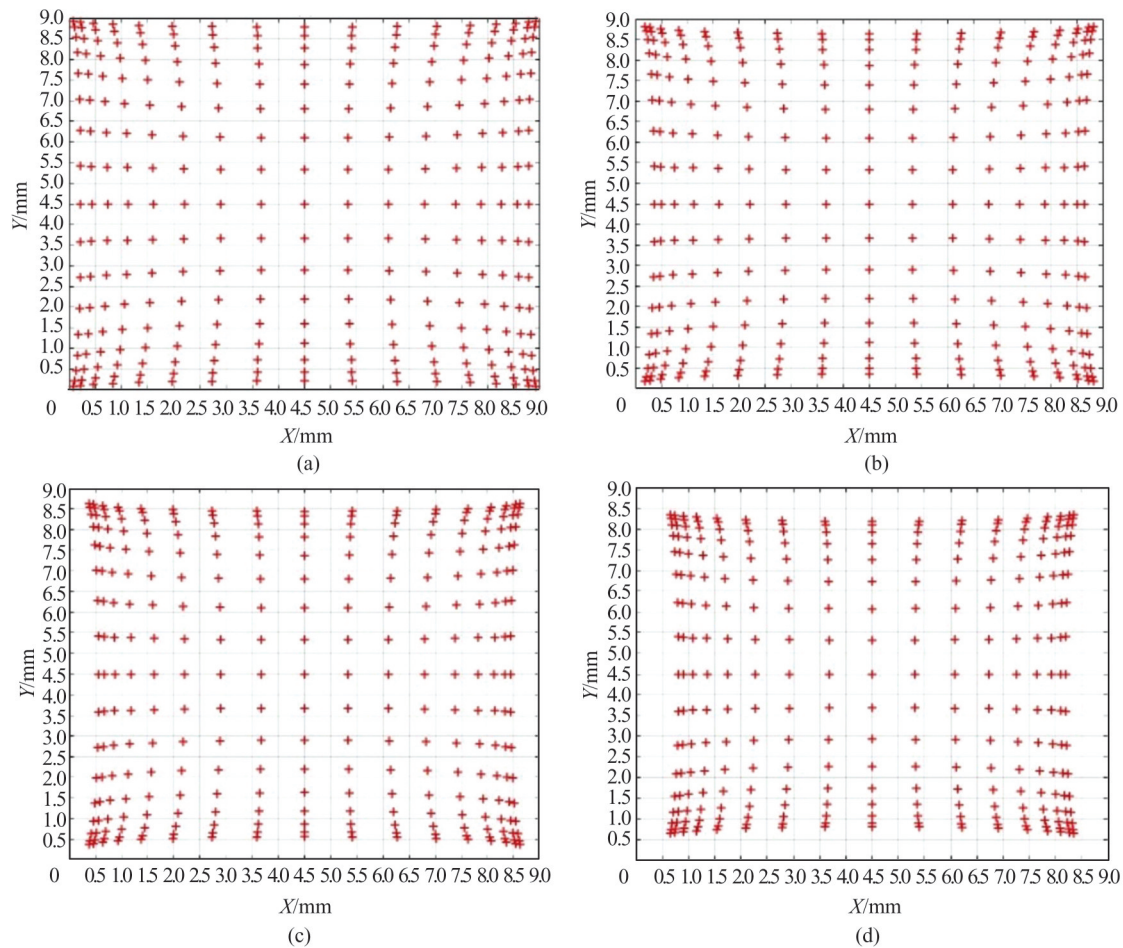


Fig. 3 Simulation of position coordinates calculation for different spot sizes

(a) at $w=0.05$; (b) at $w=0.10$; (c) at $w=0.15$; (d) at $w=0.20$.

4 Experiment

4.1 Experimental Platform

In order to investigate the impact of different spot sizes and non-linearity on positioning accuracy, a nonlinear optimization experimental platform was established, as shown in Fig. 4. The effective length of the PSD photosensitive surface is $9\text{ mm} \times 9\text{ mm}$, which is fixed on a precision displacement platform. A semiconductor laser is mounted on a three-dimensional moving platform, with adjustable spot size. By controlling the three-dimensional moving platform to scan the entire photosensitive surface of the PSD with a step size of 1 mm , a total of 100 discrete coordinate data points at 10×10 different positions were obtained. To ensure measurement accuracy, the entire experiment was conducted under dark background conditions.

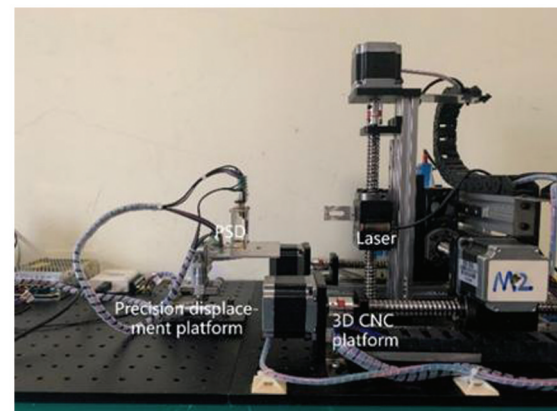


Fig. 4 Nonlinear optimization experimental platform

4.2 Algorithm Robustness

Figure 5 compares the measured coordinate data and the positions after nonlinear optimization. As seen in the figure, the actual measured positions show a pincushion distortion compared with the standardized grid.

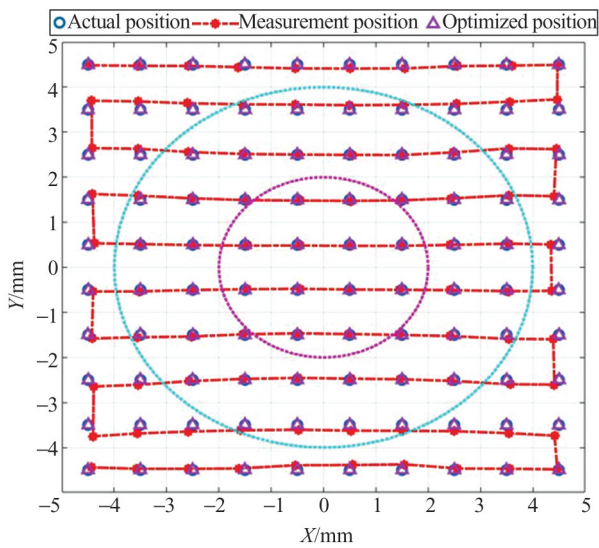


Fig. 5 Comparison of position coordinates before and after nonlinear optimization

Within Zone A, the linearity is relatively good; however, as the distance from the central point increases, significant nonlinear distortion occurs in Zone B, with the distortion being more pronounced at the four electrode ends at the outermost edges. Therefore, to extend the effective usage area of the PSD photosensitive surface while maintaining accuracy, it is necessary to correct for non-linear errors. After applying the PSO-BP correction, the linearity of the corrected positions shows a significant improvement compared with the measured positions. The comparison with the standard position coordinates visually demonstrates that the nonlinear distortion is largely eliminated.

By adjusting the laser spot diameter projected onto the photosensitive surface and collecting the measurement coordinates for different spot diameters, the comparison between the actual position coordinates and the optimized coordinates is shown in Fig. 6.

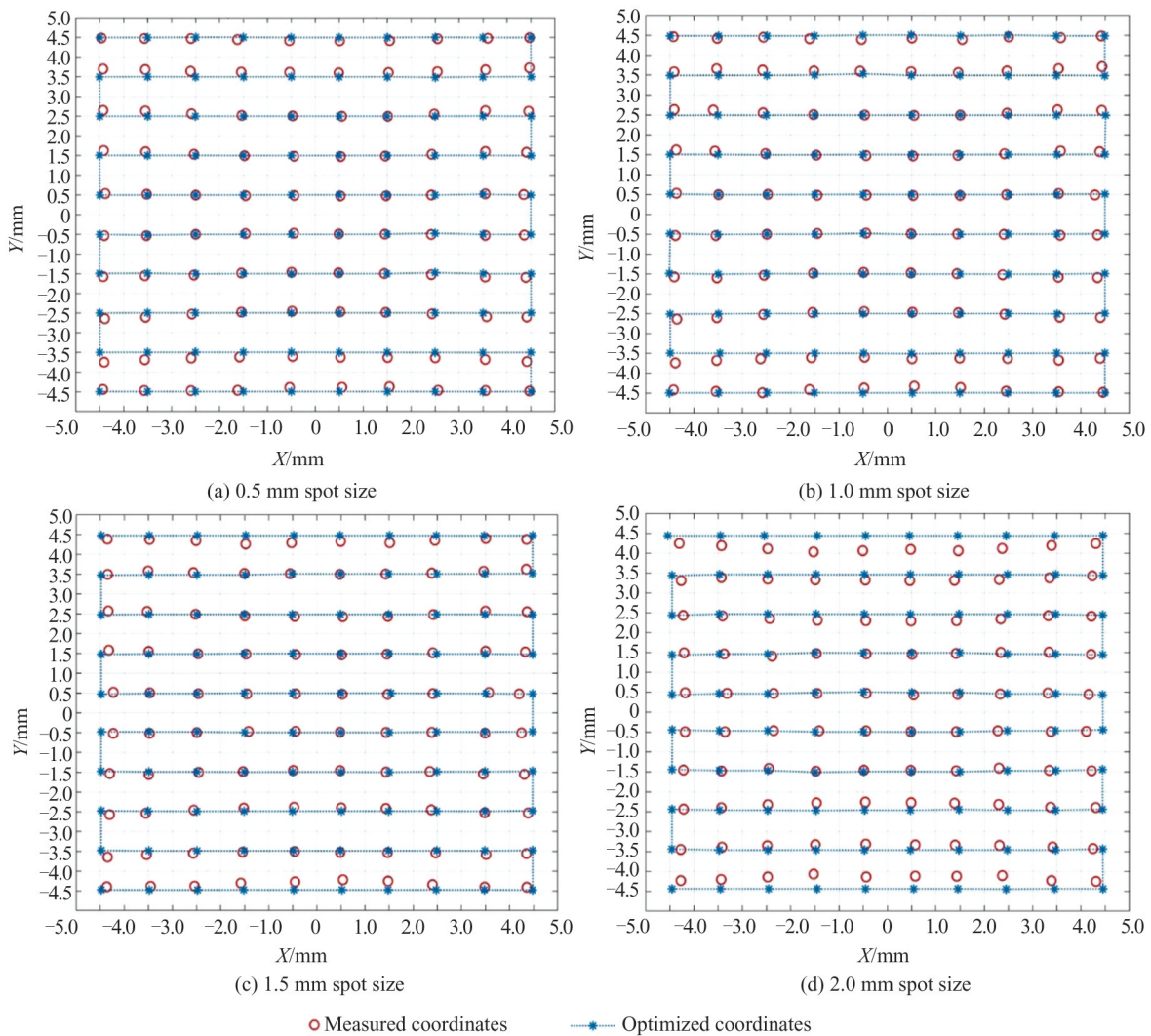


Fig. 6 Measured and optimized values for different light spots

In Fig.6, (a) , (b) , (c) , and (d) show the comparison result between the measured coordinates and the optimized coordinates for laser spots with diameters of 0.5 mm, 1.0 mm, 1.5 mm, and 2.0 mm, respectively. It can be observed that as the spot diameter increases, the accuracy of the PSD in detecting the laser spot position decreases, and the degree of nonlinear distortion increases. However, after optimization with the PSO-BP algorithm, the linearity significantly improves.

4.3 Error Analysis

Due to the varying degrees of distortion in the Zones A and B of the photosensitive surface, the significance of nonlinear optimization is also affected. To clearly distinguish the optimization significance between the Zones A and B, we selected and compared the position coordinates of the same light spot along the same diagonal under four different spot sizes.

After nonlinear optimization of the position coordinates obtained from laser spots of various sizes on the PSD’s photosensitive surface, the error can be used to evaluate the effectiveness of linearity optimization. The optimization results for Zone A of the photosensitive surface are shown in Fig. 7. In Zone A, within 40% of the distance from the center of the photosensitive surface, linearity remains good. Under the condition of a spot size of 0.5 mm, the average error after optimization in Zone A is controlled to within 1.69 μm , achieving an optimization level of 95.19% compared with the pre-optimization error. As the spot size increases, the level of optimization gradually decreases, with errors reducing by more than 85.39% when the spot size reaches 2.0 mm.

Figure 8 shows the optimization results for Zone B of the photosensitive surface. The figure indicates that

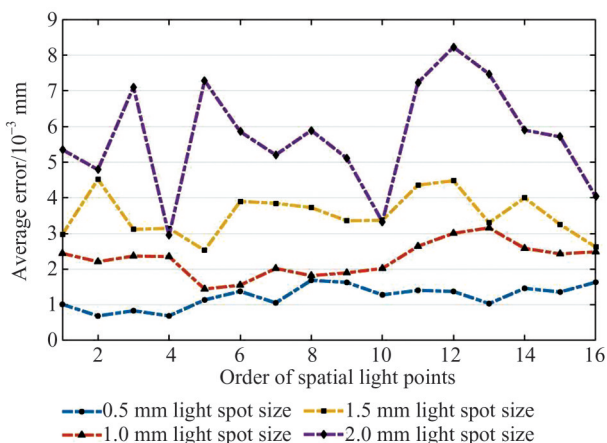


Fig. 7 Comparison of the average error of Zone A under different spot sizes

when the spot size is below 1.0 mm, the results of non-linear optimization are significant, with the average error after optimization reduced by more than 93.89%. However, when the spot size reaches 2.0 mm, the optimization effect shows a significant weakening trend, and the average error reduced by 72.58%. This indicates that smaller spot diameters result in more concentrated energy, leading to higher positioning accuracy for the PSD. Considering the nonlinear optimization results for various spot sizes across both Zone A and Zone B of the photosensitive surface, the average positioning error was reduced by 84.51% after optimization.

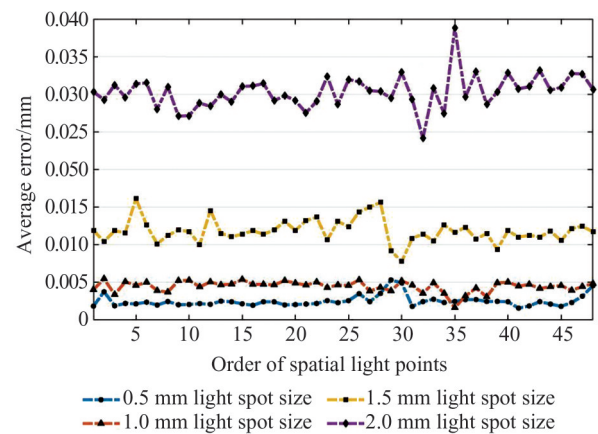


Fig. 8 Comparison of the average error of Zone B under different spot sizes

5 Conclusion

In this paper, we derived the Lucovsky differential equation mathematical model for the PSD and obtained a positioning model for the two-dimensional PSD under different spot sizes. Through simulation, we found that as the spot size increases, the positioning accuracy decreases. To address the inherent nonlinear distortion issues of the PSD, we employed a particle swarm optimization algorithm to improve the BP neural network nonlinear optimization method. The optimization significantly reduced the nonlinear errors in both the Zone A and B, effectively eliminating the pillow-shaped distortion. Moreover, the nonlinear distortion of different spot sizes projected onto the photosensitive surface was reliably corrected, with an average optimization improvement of over 84.51%, especially achieving over 93.89% for spots smaller than 1.0 mm. This greatly reduced the positioning error of the detector. Based on the research presented, the effective usable area of the photosensitive surface can be increased, and the positioning accuracy of the PSD can be enhanced,

enabling the two-dimensional PSD to be applied in wide-range and high-precision measurement systems.

References

- [1] Han J Y, Wang S Z. Research on the method of applying position sensitive detector to detect flatness[J]. *Combined Machine Tools and Automated Machining Technology*, 2016(7): 82-85(Ch).
- [2] Quan L Y, Tan J P, Wang X, *et al.* Research on real-time inspection system for high precision extrusion machine centerline coaxiality[J]. *Forging and Pressing Technology*, 2012, **37**(3): 73-77(Ch).
- [3] Lu X H, Wang W T, Si L K, *et al.* Dual PSD-based robotic motion trajectory tracking measurement device[J]. *Manufacturing Technology and Machine Tools*, 2015(6): 61-66(Ch).
- [4] Lucovsky G. Photoeffects in nonuniformly irradiated P-N junctions[J]. *Journal of Applied Physics*, 1960, **31**(6): 1088-1095.
- [5] Wang X D, Ye M Y. Nonlinear correction of two-dimensional optoelectronic position-sensitive devices[J]. *Optical Technology*, 2002(2): 174-175+178.
- [6] Shang H Y, Zhang G J. Response characteristics of PSD based on two scanning methods[J]. *Journal of Instrumentation*, 2005(11): 34-38(Ch).
- [7] Li K, Xuan R X, Zhang H M, *et al.* Influence of light source on the positioning accuracy of position-sensitive sensors[J]. *Journal of Hubei Automotive Industry College*, 2010, **24**(2): 37-40(Ch).
- [8] Huang Z H, Li X D, Cai H Y, *et al.* Research on PSD-based optical spot position detection technology in strong background[J]. *Optical Engineering*, 2012, **39**(10): 89-94(Ch).
- [9] Zhang X T, Kang L, Wu Q Q, *et al.* Nonlinear correction of PSD based on BP optimization algorithm [J]. *Journal of Applied Optics*, 2016, **37**(3): 415-418(Ch).
- [10] Wang J Y, Wang X D, Liu Z, *et al.* Nonlinear distortion correction algorithm for two-dimensional PSD[J]. *Journal of Wuhan University of Science and Technology*, 2019, **42**(1): 56-60(Ch).
- [11] Teng Y K, Hao Y M, Fu S F, *et al.* Calibration technique for position-sensitive device based visual measurement system [J]. *Advances in Laser and Optoelectronics*, 2018, **55**(8): 304-311.
- [12] Zhang P C, Liu J, Yang H M, *et al.* Research on non-uniform laser spot center localization based on PSD[J]. *Laser and Infrared*, 2020, **50**(8): 941-947(Ch).
- [13] Liu X, Liu Z, Liang Z, *et al.* PSO-BP neural network-based strain prediction of wind turbine blades[J]. *Materials (Basel)*, 2019, **12**(12): 1889.
- [14] Yu J Q, Gao Z K, Zhao A J, *et al.* Improved parallel particle swarm algorithm for energy saving optimization of cooling water systems[J]. *Control Theory and Applications*, 2022, **39**(3): 11(Ch).
- [15] Banks A, Vincent J, Anyakoha C. A review of particle swarm optimization. Part I: Background and development [J]. *Natural Computing*, 2007, **6**(4): 467-484.
- [16] Shi Y, Eberhart R. A modified particle swarm optimizer[C]// 1998 *IEEE International Conference on Evolutionary Computation Proceedings. IEEE World Congress on Computational Intelligence*. New York: IEEE, 1998: 69-73.
- [17] Meng N, Zeng J R, Li Z L, *et al.* Position detection of synchrotron light spot based on position-sensitive semiconductor optoelectronic devices[J]. *Nuclear Technology*, 2020, **43**(12): 18-26(Ch).

光斑尺寸及非线性度对 PSD 定位精度影响研究

汪泽川¹, 张振华^{1†}, 程绍伟¹, 杨海马², 黄勃¹, 刘瑾¹

1. 上海工程技术大学 电子电气工程学院, 上海 201620

2. 上海理工大学 光电信息与计算机工程学院, 上海 200093

摘要: 位置敏感探测器 (PSD) 被广泛应用于平整度检测、自准直仪系统及自由度测试等精密测量领域。然而, 由于表面电阻不均匀和电极结构差异等因素, PSD 的非线性问题在光敏表面从中心向四个电极的边缘靠近时变得越来越严重。针对这一问题, 提出了一种 PSD 非线性校正算法, 利用粒子群 (PSO) 算法计算出最佳权值和阈值, 为 BP 神经网络提供较好的初始参数, 再通过 BP 神经网络不断迭代, 直到满足误差条件, 完成校正过程。此外, 构建了 PSD 非线性校正系统, 根据高斯光斑模型条件下的电流方程, 仿真不同的光斑尺寸对 PSD 定位精度的影响, 验证了校正算法在不同光斑尺寸下的鲁棒性。结果表明, 优化后的整体误差减少了 84.51%, 当光斑尺寸小于 1mm 时, 误差减少超过 93.89%。该方法不仅满足了测量精度要求, 还扩展了 PSD 的测量范围。

关键词: 位置敏感探测器; 粒子群算法; 非线性优化; 光斑特性; 定位精度

□